

1 **Factors Contributing to Landslide Susceptibility of the Kope Formation,**
2 **Cincinnati, Ohio**
3

4 MICHAEL P. GLASSMEYER

5 Kleinfelder, 180 Sheree Boulevard, Suite 3800, Exton, PA 19341
6

7 ABDUL SHAKOOR*

8 Department of Geology, Kent State University, Kent, OH 44242
9

10 **ABSTRACT**
11

12 The objective of this study was to evaluate the factors that contribute to the high
13 frequency of landslides in the Kope Formation and the overlying colluvial soil present in the
14 Cincinnati area, southwestern Ohio. The Kope Formation consists of approximately 80% shale
15 inter-bedded with 20% limestone. The colluvium that forms from the weathering of the shale
16 bedrock consists of a low plasticity clay. Based on field observations, liDAR (light detection and
17 ranging) data, and information gathered from city and county agencies, we created a landslide
18 inventory map for the Cincinnati area, identifying 842 landslides. From the inventory map, we
19 selected ten landslides for detailed investigations that included seven rotational and three
20 translational slides. Representative samples were collected from the landslide sites for
21 determining natural water content, Atterberg limits, grain size distribution, shear strength
22 parameters, and slake durability index. For the translational landslides, strength parameters were
23 determined along the contact between the bedrock and the overlying colluvium. The results of
24 the study indicate that multiple factors contribute to landslide susceptibility of the Kope
25 Formation and the overlying colluvium including low shear strength of the colluvial soil,
26 development of porewater pressure within the slope, human activity such as loading the top or
27 cutting the toe of a slope, low to very low durability of the bedrock that allows rapid
28 disintegration of the bedrock and accumulation of colluvial soil, undercutting of the slope toe by
29 stream water, and steepness of the slopes.

30 Key Terms: *Kope Formation, Colluvial Soil, Landslide Susceptibility, Shear Strength, Pore*
31 *Pressure, Slake Durability, Toe Undercutting.*

32
33 *Corresponding Author: Abdul Shakoor – ashakoor@kent.edu

34 35 INTRODUCTION

36 Landslide Problem in the Cincinnati Area

37 The Cincinnati area (Hamilton and Clermont counties) comprises the southwestern corner
38 of Ohio and is one of the most landslide susceptible areas in the United States [Ohio Emergency
39 Management Agency (EMA), 2011]. Most of the landslides occur in the Kope Formation and the
40 overlying colluvial soil during late winter and early spring (Fleming, 1975). Landslide damage
41 and mitigation cost the city millions of dollars each year (Rockaway, 2002). According to
42 Schuster (1996), the annual per capita cost for landslide damage in the Cincinnati area was \$5.80
43 in 1981 (equivalent to \$17.27 in 2020). This does not include more than \$22 million spent in
44 1981 (equivalent to \$65.5 million in 2020) to stabilize a single landslide that occurred on Mount
45 Adams during the construction of Interstate 471. One of the costliest time periods for landslide
46 damage in the Cincinnati area occurred between 1973 and 1978 when, over a six-year period, an
47 average of \$5.1 million in 1981 dollars (equivalent to \$15.2 million in 2020) was spent per year
48 to repair landslide damage (Schuster, 1996).

49 Rotational and translational slides are the most frequently occurring slope movements
50 associated with the Kope Formation and the overlying colluvial soil. Rapid earthflows, rockfalls,
51 and complex slides (combination of rotational and translational slides), although present, are
52 infrequent. Rotational slides are common where thick colluvium covers the bedrock. They are
53 generally 2-15 m thick, 30-300 m wide (measured perpendicular to the direction of sliding), and
54 30 -150 m long (measured along the direction of sliding). Many rotational slides are associated
55 with springs or marshy areas either beneath or within the slope toes (Fleming and Johnson,

56 1994). Translational slides are common where thin colluvial soils (2-3 m thick) cover relatively
57 steep slopes (15°-30°). They occur along the colluvium-bedrock contact, are generally 10-150 m
58 wide and 30–130 m long, and they vary in shape from long and narrow to wide and short
59 (Richards, 1982). Translational slides generally occur during spring because the slide material is
60 almost saturated between the months of January and May (Haneberg, 1991; 1992; Haneberg and
61 Gokce, 1994). The dominant form of deformation in translational slides is longitudinal stretching
62 resulting in a series of scarps. Complex landslides in the Cincinnati area consist of more than one
63 layer of slide material. They are thinner near the slope crest and become thicker near the toe.
64 Rapid earth flows in the Kope Formation (locally known as mudslides) occur on steeper slopes
65 along the Columbia Parkway. They occur during wet periods in areas where the colluvium is < 2
66 m thick and is clayey in nature (Pohana, 1983). Rapid earthflows involve movement of the entire
67 thickness of the colluvium, exposing the bedrock (Richards, 1982; Riestenberg and Sovonik-
68 Dunford, 1983)

69 Geology of the Cincinnati Area

70 The Cincinnati area forms the western flank of the Cincinnati Arch where the bedrock
71 dips gently at less than 1° (Fleming, 1975). The area represents an upland surface, enveloped by
72 the Pre-Illinoian, Illinoian, and Wisconsinan age glacial deposits, that has been dissected by
73 ancient drainage systems as well as the modern Ohio River and its tributaries (Pavey et al., 1992;
74 Potter, 2007). Many of the tributaries have carved broad, terraced valleys with steep slopes. The
75 relief between the Ohio River and the hilltops in the area is approximately 120 m (Baum and
76 Johnson, 1996). Alluvium and glacial outwash cover the valley floors and colluvium covers most
77 of the hillsides (Baum and Johnson, 1996).

78 The Kope Formation in the Cincinnati area is overlain by the Fairview Formation, both

79 being Upper Ordovician in age. The contact between the two formations is at an elevation
80 between 200 and 215 m (Gibbons, 1973). Figure 1 shows the extent of the Kope Formation in
81 the Cincinnati area, as indicated by the surficial geology map. The formation is more than 60 m
82 thick and consists of inter-bedded, medium to dark grey, shale (80%) and coarse-grained
83 fossiliferous limestone (20%) (Fleming and Johnson, 1994). It should be noted that what is
84 referred to as “shale” in the earlier studies is mudstone/claystone according to Potter et al. (1980)
85 classification (Sarman, 1991; Dick, 1992; Hajdarwish, 2006). The shale (mudstone/claystone)
86 consists of illite, chlorite, calcite, and quartz (Sarman, 1991; Dick, 1992; Hajdarwish, 2006). The
87 limestone layers within the Kope Formation contain three sets of near-vertical joints, occurring at
88 regular spacing. The orientations of the joints, however, vary between different locations
89 (Hofman, 1966; Brett and Algeo, 2001; Brett et al., 2003). The shale also contains steeply
90 dipping joints (Richards, 1982; Baum, 1983). The colluvium associated with the Kope Formation
91 classifies as Eden silty clay loam according to the Hamilton County Soil Survey Report and as
92 clay of low plasticity (CL) according to the Unified Soil Classification System (USCS) (Lerch et
93 al., 1982; Glassmeyer, 2014). The colluvium covers most of the hillsides and generally ranges in
94 thickness from a few centimeters up to 15 m (Fleming and Johnson, 1994), but can be much
95 thicker at some places.

96 Study Objectives

97 Although landslides in the Cincinnati area have been studied extensively, a specific and
98 detailed study regarding the susceptibility of the Kope Formation to landslide occurrence has not
99 been conducted. Thus, the main objective of this study was to investigate the factors that
100 contribute to high landslide susceptibility of the Kope Formation and the colluvium derived from
101 it (Note: in this study, the colluvium is synonymous to the Kope Formation). This objective was

102 accomplished by performing the following tasks:

- 103 1. Create a landslide inventory map for the Kope Formation and the associated colluvium.
- 104 2. Determine the engineering properties of the Kope Formation and the overlying
105 colluvium.
- 106 3. Identify the types of slope movement that affect the Kope Formation.
- 107 4. Explain the landslide susceptibility of the Kope Formation and the overlying colluvium in
108 terms of engineering properties, slope characteristics, and hydrologic conditions.

109 RESEARCH METHODS

110 Landslide Inventory

111 We developed a landslide inventory map for the Kope Formation and the overlying
112 colluvial soil using LiDAR (light detection and ranging) data, field observations, and landslide-
113 locations data from city and county governments (Figure 2). A total of 842 landslides were
114 identified in the colluvial soil derived from the Kope Formation. Of these, 542 landslides were
115 identified using the LiDAR-derived maps and 300 were identified through field observations and
116 data obtained from city and county governments. The LiDAR data, with an accuracy of 0.33 m,
117 was divided into tiles that were 1524 m by 1524 m square. Since the LiDAR data is a las (a blob
118 point file or a collection of binary data stored as a single entity), the data were converted into
119 usable maps using ArcGIS. The files were first converted from multipoint files to ASCII files.
120 The ASCII files were then converted to raster files. Once the raster files were created, we
121 developed a slope map, a hillshade map, a digital elevation map (DEM), and a topography map
122 for the study area. These maps were used to identify landslide related features such as scarps and
123 toe bulges. Randomly selected landslides from the inventory map were verified through field
124 observations, using the GPS. Before mapping the landslides, three different layers were used to

125 define the area of interest on LiDAR-derived maps: (i) the extent of the Kope Formation in the
126 Cincinnati area as defined by the Ohio Department of Natural Resources (ODNR) bedrock
127 geology map, (ii) the extent of the Kope Formation as defined by the ODNR surficial geology
128 map, and (iii) the extent of the colluvium as defined by the ODNR soil survey division.

129 Site Selection, Data Collection, and Sampling for Detailed Investigations

130 From the landslide inventory map, we selected ten landslide sites for detailed
131 investigations (Figure 3). These included seven rotational landslide sites (Eight Mile Road
132 landslide, Ten Mile Road landslide, Delhi Pike landslide complex, Elstun Road landslide,
133 Nordyke Road landslide, Old US 52 landslide, Wagner Road landslide) and three translational
134 landslide sites (Nine Mile Road landslide, Berkshire Road landslide, Columbia Parkway
135 landslide). The selected sites represented a range of landslide sizes and geographic locations. The
136 data collected at each site included slope geometry (slope height, slope angle, and slope length),
137 thickness of the colluvium, type of slope movement, location of the failure plane with respect to
138 slope face, whether the slide occurred in the colluvium or within the bedrock, and landslide
139 dimensions (length and width). Where possible, information about the hydrogeologic conditions
140 was obtained. We used Cruden and Varnes classification system (Cruden and Varnes, 1996) to
141 identify the type of slope movement at each site. For describing landslide features and for
142 measuring landslide dimensions at different sites, we used the standardized terminology
143 recommended by the International Association of Engineering Geology (IAEG) Commission on
144 Landslides (IAEG, 1990). Undisturbed chunk samples of colluvial soil, weighing approximately
145 5 kg, were collected from each site for laboratory testing. Additionally, bedrock samples were
146 collected from the three translational landslide sites. The samples were immediately sealed in air-
147 tight bags and stored in five-gallon plastic buckets to preserve natural water content of the soil

148 samples and to prevent slaking of the bedrock samples.

149 Laboratory Investigations

150 Laboratory tests were conducted to determine natural water content, grain size
151 distribution, Atterberg limits, shear strength parameters, and slake durability index. All tests
152 were performed following the American Society for Testing and Materials (ASTM)
153 specifications (ASTM, 2010). Natural water content, an indicator of the soil's void ratio, was
154 determined as soon as the soil samples were brought to the laboratory. Both sieve analysis and
155 hydrometer analysis were used to determine the grain soil distribution of the colluvial soil
156 samples. The results of grain size distribution analysis helped classify the soil from each site
157 according to the Unified Soil Classification System (USCS) (Casagrande, 1948; Holtz et al.,
158 2011). Atterberg limits test was performed only on material passing the #200 sieve (0.074 mm)
159 to determine liquid limit, plastic limit, and plasticity index. The test results were used to classify
160 the fine-grained fraction of the soil according to the USCS. Two versions of the direct shear test
161 were conducted to determine shear strength parameters. The purpose of the first version was to
162 simulate failure conditions in case of rotational landslides with the failure plane located entirely
163 within the soil whereas the second version simulated the failure conditions for the translational
164 slides with the failure occurring along the contact between the bedrock and the overlying
165 colluvial soil. The slake durability test was performed on the bedrock samples that were
166 collected from the Nine Mile Road landslide, Berkshire Road landslide, and Columbia Parkway
167 landslide sites where the bedrock is at shallow depths. The purpose of the slake durability test
168 was to evaluate weathering potential of the bedrock. Two cycles of the test were performed on
169 each sample and the 2nd-cycle slake durability index (Id_2) was calculated. Based on Id_2 values,
170 and using the International Society for Rock Mechanics (ISRM) classification (ISRM, 2007), the

171 durability of the samples was classified as follows: high ($I_d > 95\%$); medium ($I_d = 85\%-95\%$);
172 low durability ($I_d = 60\%-85\%$); and very low durability ($I_d = 0\%-60\%$).

173 Stability Analysis

174 The computer program Slide 6.0 (Rocscience, 2012) was used to perform stability
175 analysis for the ten sites. The program identified the critical surface of failure and calculated the
176 corresponding factor of safety (FS) for both dry and saturated conditions. We also used Slide to
177 perform sensitivity analysis, i.e. variation of FS with respect to strength parameters and
178 groundwater conditions.

179 RESULTS

180 Laboratory Test Results

181 The natural water content values for the colluvial soils from the ten landslides sites range
182 from 13.1% to 27.1%, with a mean value of 20.4% (Table 1). The relatively high water content
183 values suggest the presence of a high percentage of fine-grained clayey material in the colluvial
184 soils at the landslide sites. This implies that even a small amount of precipitation can result in
185 buildup of pore pressure and reduction in shear strength, leading to failure. The high water
186 content values also indicate the potential for flow type movement.

187 The results of grain size distribution analysis indicated that, according to USCS, colluvial
188 soils derived from the Kope Formation classify as clayey sand (SC). It should be noted that
189 although the colluvial soil classifies as clayey sand, the sand size particles consist of broken
190 pieces of shale bedrock and fossils, overall, the colluvium behaves as a clay of low plasticity
191 during landslide activity.

192 Table 2 presents the Atterberg limits test results for the fine-grained fraction of the
193 colluvium from the ten sites. A plot of Atterberg limits on Casagrande plasticity chart is shown

194 in Figure 4. The plot shows that the fine-grained fraction of the colluvial soil classifies as clay of
195 low plasticity (PL). Table 2 also lists the liquidity index (LI) values. The liquidity index
196 compares the natural water content with the Atterberg limits and indicates how a soil will behave
197 when sheared. If LI is > 1 , the soil will behave as a viscous liquid when sheared, if it ranges from
198 0-1, the soil will behave as a plastic material on shearing, and if it is < 0 , the soil will behave as a
199 brittle material. The LI values in Table 2 indicate a plastic behavior of colluvial soil during
200 landsliding.

201 The strength parameters of a soil (cohesion and friction angle) are the most important
202 engineering property of a soil in terms of the stability of a slope. For the soil alone (rotational
203 slides scenario), the peak cohesion and friction angle range from 24.5 kPa to 47.7 kPa and 22.8°
204 to 39.4° , respectively, and the residual cohesion and friction angle from 22.2 kPa to 38.9 kPa and
205 residual friction angle from 15.6° to 20.8° (Table 3). For soil-bedrock contact (translational slide
206 scenario), the residual cohesion ranges from 6.8 kPa to 13.0 kPa, and the residual friction angle
207 from 8.0° to 14.6° (Table 4) We provide only residual strength parameters for soil-bedrock
208 contact because of the slow, continual movement of the thin soil layer over bedrock. These shear
209 strength parameter values are inadequate to maintain stability with respect to both rotational and
210 translational slides.

211 The second cycle slake durability index (Id_2) ranges from 7.1% (very low durability) for
212 the Columbia Parkway landslide to 39.9% (low durability) for the 9 Mile Road landslide (Table
213 5). The low to very low durability of the Kope Formation explains the thick accumulation of
214 colluvial soil at many locations. The durability properties of argillaceous rocks are important in
215 slope stability because of the reduction in strength properties as a result of weathering (Dick and
216 Shakoor, 1995).

217 Stability Analysis Results for Selected Slope Failures

218 Rotational landslides constitute the most common type of slope failure in the colluvial
219 soil derived from the Kope Formation. All seven rotational landslides that were studied in detail
220 occurred in colluvial soil. Rotational landslides occur where the colluvial soil is > 3 m thick.

221 Translational landslides are the second most common type of failure in the colluvial soil.
222 Translational landslides tend to occur in complexes, affecting wide-spread areas. The failure
223 plane for a translational slide is located along the contact between the colluvial soil and the
224 underlying bedrock. The sliding mass for the three translational slides studied (Nine Mile Road
225 landslide, Berkshire Road landslide, Columbia Parkway landslide) consists of colluvial soil. The
226 thickness of colluvial soil at the locations of translational slides was found to be approximately
227 1.5 m to 3.0 m. Detailed descriptions of both rotational and landslides can be found in
228 Glassmeyer (2014)

229 For the sake of brevity, we present stability analysis for one rotational landslide (Ten
230 Mile Road landslide) and one translational landslide (Columbia Parkway landslide). For stability
231 analyses for all ten landslides, see Glassmeyer (2014). The software program Slide (Rocscience,
232 2012) was used to perform the stability analysis, using residual strength parameters. For the Ten
233 Mile Road landslide (Figure 5), the critical surface with the lowest factor of safety (FS) is shown
234 in Figure 6, which matches the failure surface location observed in the field (Figure 5). The Slide
235 program resulted in a FS of 0.83 for the dry condition and 0.79 for the saturated condition. The
236 stability analysis indicated that for the FS to be >1, the cohesion of the soil should be > 61.2 kPa
237 (instead of 22.5 kPa) if the friction angle were to remain constant at 15.6°, or the friction angle
238 needs to be > 33.8° if the cohesion remains the same (22.5 kPa) (Table 3).

239 For the Columbia Parkway landslide (Figure 7), the critical surface, as determined by the

240 Slide program, is located along the contact between the colluvial soil and the underlying bedrock
241 (Figure 8). It initiates at the top of the slope and emerges at the top of the retaining wall at the
242 base of the slope (Figure 7). It should be noted that soil-bedrock contact may not be perfectly
243 planar (Figure 8) but we assumed it to be planar for the purpose of stability analysis. Also, we
244 assumed a uniform, average colluvium thickness. Locally, the landslide may change into
245 earthflow/mudflow. The minimum FS for the dry condition is 1.04, when the colluvium is dry,
246 and 0.68 when saturated. Stability analysis results show that the soil-rock friction angle needs to
247 be $>18^\circ$ instead of 14.8° (Table 4) for the FS to be >1 , if the cohesion were to remain constant at
248 6.8 kPa, or the cohesion should be >8.9 kPa if the friction angle remains constant (14.8°) (Table
249 4). These results clearly suggest that strength parameters of the colluvial soil are lower than those
250 required to maintain stability.

251 The Columbia Parkway landslide is currently being stabilized at an estimated cost of \$17
252 million (City of Cincinnati – Transportation & Engineering, 2020). The stabilization project
253 extends from Bains Street (Mt. Adams area) on the west side to beyond Torrence Parkway (East
254 Walnut Hills area) on the east side, a nearly two-mile long stretch of the Parkway. Within this
255 stretch, 12 landslide locations have been chosen for stabilization with the stabilization method,
256 involving either metal mesh and soil nails or retaining walls (Figure 9), varying from location to
257 location (City of Cincinnati – Transportation & Engineering, 2020). The construction started
258 towards the end of 2019 and is expected to be completed by summer 2021 (City of Cincinnati –
259 Transportation & Engineering, 2020).

260 FACTORS CONTRIBUTING TO LANDSLIDE SUSCEPTIBILITY 261 OF THE KOPE FORMATION 262

263 *Low Shear Strength*

264 We believe the residual strength parameters are more important than the peak strength

265 parameters for the long-term stability of slopes comprised of colluvial soil derived from the
266 Kope Formation. This is because many of the landslides in the Kope Formation develop
267 progressively over a long period of time. Figures 10 and 11 show the relationships between
268 factor of safety and the residual strength parameters for the Ten Mile Road and Columbia
269 Parkway landslides, respectively. A comparison of these plots with the residual strength
270 parameters (Tables 3 and 4) shows that the residual cohesion and residual friction angle values
271 for both rotational and translational slides are not high enough to support the slopes (i.e. the
272 values in the tables are lower than those required to provide a $FS > 1$). Therefore, the low shear
273 strength of the colluvial soil and soil-bedrock contact is an important factor contributing to
274 landslide susceptibility of the Kope Formation.

275 *Porewater Pressure*

276 The presence of water within a slope can significantly decrease the stability of a slope.
277 The average amount of precipitation in the Cincinnati area is 107 cm (US Climate Data, 2014).
278 Since the colluvial soil classifies as a clayey sand for all landslides studied, it can be assumed
279 that the material has low permeability and poor drainage characteristics (Holtz et al., 2011). This
280 can lead to buildup of porewater pressure within the slope during prolonged periods of rainfall
281 and snow melt, reducing shear strength and contributing to slope failure. Figure 12 shows the
282 relationship between the location of the water table and the FS for the slopes at the Ten Mile
283 Road and Columbia Parkway landslide sites. In this figure, 0 (along the vertical axis) represents
284 the water table located at the bedrock level and 1 represents the water table at the ground surface,
285 and values in between represent the relative elevations of the water table from the bedrock to the
286 ground surface. The plots in Figure 12 show that, as the water table within the slope rises, the FS
287 of the slope gradually decreases. The FS is at its lowest value when the water table is at the

288 ground surface. i.e. the soil is completely saturated. Only a partial saturation of the colluvial
289 slopes is required to cause failure, as several other factors also contribute to instability. Many of
290 the slopes in the study area show either continually flowing water or water seeps throughout the
291 year. Thus, development of pore pressure is another important factor that explains the high
292 susceptibility of the Kope Formation to landsliding.

293 *Human Activity*

294 Human activity is an important factor influencing the stability of many slopes in the
295 Cincinnati area (Behringer, 1992). Construction activities alter the stability of a slope in two
296 ways: (i) by adding weight to the top of the slope, and (ii) by removing lateral support at the toe
297 of the slope. Due to the topography of the Cincinnati area, many of the roads are built on tops of
298 hillsides, cut into hillsides, or built in the toe areas by partial removal of the slope toes. By
299 building on top of a slope, the driving forces acting on the slope increase and tend to cause
300 failure. By cutting out the hillsides and the toes of the slopes, the resisting forces decrease.

301 *Low to Very Low Durability of the Bedrock*

302 The Kope Formation is a clay-bearing rock of low to very low durability against slaking
303 ($Id_2 = 7.1\% - 39.9\%$) because of which it easily disintegrates and erodes rapidly. It is the easy
304 disintegration of the Kope Formation that leads to thick accumulation of the colluvial soil on top
305 of bedrock. The nondurable nature of the Kope Formation and the colluvial soil derived from it
306 make these materials susceptible to landsliding.

307 *Undercutting of the Slope Toe*

308 Many slopes in the Cincinnati area are subject to undercutting of the slope toe by stream
309 erosion (Figure 5). This removes the lateral support, thereby reducing the resisting forces.
310 Undercutting of the slope toe, facilitated by the low durability of the Kope Formation, is a very

311 important factor contributing to high susceptibility of the Kope Formation to landsliding.

312 *Steepness of Slopes*

313 The steepness of natural slopes in the Cincinnati area is another contributing factor to
314 landslide susceptibility of the colluvium that is associated with the Kope Formation. The low to
315 very low durability of the bedrock results in rapid down cutting of the valleys, giving rise to
316 steep slopes. Although the bedrock slopes may reach a state of equilibrium at relatively steeper
317 angles, the colluvial soils that cover the bedrock are not strong enough to maintain stability at
318 those angles. Furthermore, many slopes have been over-steepened because of the rapidly eroding
319 streams or human activity. The slope angles in the Cincinnati area range between 20° and 40°,
320 which is generally higher than the residual friction angle values. The results of the stability
321 analysis show that slopes steeper than 15° will not have an adequate factor of safety against
322 failure under wet conditions.

323 The above discussion shows that multiple factors, either individually or in combination,
324 contribute to the high susceptibility of the Kope Formation to landsliding.

325 CONCLUSIONS

326 Based on the results of this study, the following conclusion can be drawn:

- 327 1. Rotational and translational landslides are the main types of movement affecting the
328 slopes comprised of colluvial soil derived from the Kope Formation. Once a failure has
329 been initiated, both types of movement may transform into earthflows, and occasionally
330 into mudflows, with the addition of water.
- 331 2. The factors that contribute to the high susceptibility of the colluvial soil to landslides
332 include low shear strength parameters of the soil or soil/bedrock contact, development of
333 porewater pressure, human activity, low to very low durability of the bedrock,

334 undercutting of the slope toe by stream water, and steepness of the slopes.

335

336

REFERENCES

337

338 AMERICAN SOCIETY FOR TESTING AND MATERIALS (ASTM), 2010, Annual Book of
339 Standards: Section 4, Construction, 4.08, Soil and Rock (1), Conshohocken, PA.

340

341 BAUM R.L., 1983, Engineering geology and relative slope stability in the area of the Fay
342 Apartments and in part of Mount Airy Forest, Cincinnati, Ohio: MS Thesis, University of
343 Cincinnati, Cincinnati, OH, 74 p.

344

345 BAUM R.L. AND JOHNSON, A.M., 1996, Overview of landslide problem, research, and
346 mitigation, Cincinnati, Ohio, Area: U.S. Geological Survey Bulletin 2059-D, Washington
347 DC, United States Government Printing Office, 33 p.

348

349 BEHRINGER, D.W., 1992, A Study of Selected Landslides in the Cincinnati Area in Relation to
350 Human Activity: MS Thesis, Kent State University, Kent, OH, 164 p.

351

352 BRETT, C. E. AND ALGEO, T.J., 2001, Stratigraphy of the Upper Ordovician Kope Formation
353 in its type area (northern Kentucky), including a revised nomenclature: In Algeo, T.J. and
354 Brett, C.E. (editors), Sequence, cycle and event stratigraphy of the Upper Ordovician and
355 Silurian strata of the Cincinnati Arch region., Kentucky Geological Survey, series 12,
356 Guidebook 1, pp. 47-64.

357

358 BRETT, C.E., ALGEO, T.J., AND MCLAUGHLIN, P.J., 2003, Use of event beds and
359 sedimentary cycles in high resolution stratigraphic correlation of lithologically repetitive
360 successions: The Upper Ordovician Kope Formation of northern Kentucky and
361 southwestern Ohio: In Harries, P. (editor), High-resolution approaches in stratigraphic
362 palaeontology. Amsterdam, Plenum Press, pp. 315-350.

363

364 CASAGRANDE, A., 1948, Classification and identification of soils: Transactions, American
365 Society of Civil Engineers (ASCE), Vol. 113, pp. 901-930.

366

367 CITY OF CINCINNATI - TRANSPORTATION & ENGINEERING / PROJECTS /
368 COLUMBIA PARKWAY HILLSIDE STABILIZATION, 2020, [https://www.cincinnati-
369 oh.gov/dote/dote-projects/columbia-parkway-hillside-stabilization/](https://www.cincinnati-oh.gov/dote/dote-projects/columbia-parkway-hillside-stabilization/).

370

371 CRUDEN D.M. AND VARNES D.J., 1996. Landslide types and processes. In Landslides:
372 Investigation and Mitigation, Turner A.K. and Schuster R.L. (Editors), Special Report 247,
373 Transportation Research Board, Washington DC, pp. 36-75.

374

375 DICK, J.C., 1992, Relationship Between Durability and Lithologic characteristics of mudrocks:
376 Ph.D. dissertation, Kent State University, Kent, OH, 243 p.

377

378 DICK, J.C. AND SHAKOOR, A., 1995, Characterizing durability of mudrocks for slope stability

379 purposes: Reviews in Engineering Geology, Geological Society of America, Vol. 10, pp.
380 121-130.
381

382 FLEMING, R.W., 1975, Geologic perspectives - The Cincinnati example: Ohio Valley Soils
383 Seminar Proceedings, Ft. Mitchell, KY., 22 p.
384

385 FLEMING, R.W. AND JOHNSON, A.M., 1994, Landslides in colluvium: U.S. Geological
386 Survey Bulletin 2059-D, Washington DC, United States Government Printing Office, 24 p.
387

388 GIBBONS, A.B., 1973, Geologic map of parts of the Newport and Withamsville Quadrangles,
389 Campsville and Kenton Counties, Kentucky, Washington DC., United States Geologic
390 Survey.
391

392 GLASSMEYER, M.P., 2014, Geological and Geotechnical Factors Responsible for Landslide
393 Susceptibility of the Kope Formation in Cincinnati, Ohio: MS Thesis, Kent State
394 University, Kent, OH, 196 p.
395

396 HAJDARWISH, A., 2006, Geologic Controls of Shear Strength Behavior of Mudrocks, Ph.D.
397 dissertation, Kent State University, Kent, OH, 258 p.
398

399 HANEBERG, W.C, 1991, Observation and analysis of pore pressure fluctuations in a thin
400 colluvium landslide complex near Cincinnati, Ohio: Engineering Geology, Vol. 31, pp.
401 159-184.
402

403 HANEBERG, W.C, 1992, A mass balance model for the hydrologic response of fine-grained
404 hillside soils to rainfall: Geological Society of America Abstracts with Programs, Vol. 24,
405 No. 7, p. 203.
406

407 HANEBERG, W.C. AND GÖKCE, A.Ö., 1994, Rapid water-level fluctuations in a thin
408 colluvium landslide west of Cincinnati, Ohio: U.S. Geological Survey Bulletin 2059-C,
409 Cincinnati, OH, 16 p.
410

411 HOFMAN, H.J., 1966, Deformational structures near Cincinnati, Ohio: Geological Society of
412 America Bulletin, Vol. 77, No. 5, pp. 533-548.
413

414 HOLTZ, R.D., KOVACS, W.D., AND SHEAHAN, T.C., 2011, An Introduction to Geotechnical
415 Engineering: Second Edition, Prentice-Hall, Inc., 853 p.
416

417 INTERNATIONAL ASSOCIATION OF ENGINEERING GEOLOGY (IAEG) COMMISSION
418 ON LANDSLIDES, 1990, Suggested nomenclature for landslides: Bulletin of the
419 International Association of Engineering Geology, No. 41, p. 13-16.
420

421 INTERNATIONAL SOCIETY FOR ROCK MECHANICS (ISRM), 2007, The Complete ISRM
422 Suggested Methods for Rock Characterization, Testing, and Monitoring: 1974-2006. In
423 Ulusay, R. and Hudson, J.A. (editors), Suggested Methods Prepared by the Commission on
424 Testing Methods, ISRM, Ankara, Turkey, 628 p.

425
426 LERCH, N.K., HALE, W.F., AND LEMASTER, D.D., 1982, Soil Survey of Hamilton County,
427 Ohio, U.S. Soil Conservation Service, 219 p.
428
429 OHIO EMERGENCY MANAGEMENT AGENCY (OHIO EMA), 2011, State of Ohio
430 Emergency Hazard Mitigation Plan: Ohio Department of Public Safety, 345 p.
431
432 PAVEY, R.R., GOLDTHWAIT, R.P., BROCKMAN, C.S., HULL, D.N., AND VAN HORN,
433 R.G., 1992, The new Quaternary map of Ohio: Geological Society of America Abstracts
434 with Programs, Vol. 24, No. 7, p. 314.
435
436 POHANA, R. E., 1983, The Engineering geologic and relative stability analysis of a portion of
437 Anderson Township, Cincinnati, Ohio: M.S. Thesis, University of Cincinnati, Cincinnati,
438 OH, 132 p.
439
440 POTTER, P.E., 2007, Exploring the geology of the Cincinnati/Northern Kentucky region:
441 Kentucky Geological Survey Special Publication 8, Series 12, KY, 128 p.
442
443 POTTER, P.E., MAYNARD, J.B., AND PRYOR, W.A., 1980, Sedimentology of Shale:
444 Springer-Verlag, New York, 310 p.
445
446 RICHARDS, K.A., 1982, The Engineering geology and relative stability of Mt. Adams, and
447 parts of Walnut Hills and Columbia Parkway, Cincinnati, Ohio: MS Thesis, University of
448 Cincinnati, Cincinnati, OH, 111 p.
449 RIESTENBERG, M.M. AND SOVONIK-DUNFORD, S., 1983, The role of woody vegetation
450 in stabilizing slopes in the Cincinnati area, Ohio: Geological Society of America Bulletin,
451 Vol. 94, pp. 506-518
452
453 ROCKAWAY, J., 2002, Southwestern Ohio Landslide Documentation Investigation Report:
454 United States Geological Survey, Denver, pp. 2 - 3.
455
456 ROCSCIENCE, 2012, Slide 6.0, <http://www.rocscience.com/products/8/Slide>
457
458 SARMAN, R., 1991, A multiple regression approach to predict swelling in mudrocks, Ph.D.
459 Dissertation, Kent State University, Kent, OH, 365 p.
460
461 SCHUSTER, R.L., 1996, Socioeconomic significance of landslides: In Landslides: Investigation
462 and Mitigation, Turner A.K. and Schuster R.L. (Editors), Special Report 247,
463 Transportation Research Board, Washington DC, pp. 12-35.
464
465 US CLIMATE DATA, 2014, [https://www.usclimatedata.com/climate/cincinnati/ohio/united-](https://www.usclimatedata.com/climate/cincinnati/ohio/united-states/usoh0188)
466 [states/usoh0188](https://www.usclimatedata.com/climate/cincinnati/ohio/united-states/usoh0188).
467
468
469

List of Figures and Tables

470
471
472
473
474
475
476
477
478
479
480
481
482
483
484
485
486
487
488
489
490
491
492
493
494
495
496
497
498
499
500
501
502
503
504
505
506
507
508
509
510
511
512
513
514
515

Figures

Figure 1: Map showing the extent of the Kope Formation (darker brown) in the Cincinnati area. The blue star indicates the location of downtown Cincinnati. The shaded area in the south west corner of the Ohio map shows Hamilton (left) and Clermont (right) counties.

Figure 2: Landslide inventory map for the Kope Formation and the overlying colluvial soil within the Cincinnati area.

Figure 3: Locations of the landslide sites selected for detailed study.

Figure 4: Plot of Atterberg limits of the fine-grained fraction of the colluvial soils from the landslide sites on the Casagrande plasticity chart.

Figure 5: The Ten Mile Road landslide with well-developed head scarp. Notice the undercutting of the toe by a stream.

Figure 6: Critical surface for the minimum factor of safety for dry and saturated conditions for the Ten Mile Road landslide, as determined by the Slide program.

Figure 7: (a) Head scarp of the Columbia Parkway landslide and (b) toe of the Columbia Parkway landslide emerging on the top of the retaining wall.

Figure 8: Critical Surface for the minimum factor of safety for the Columbia Parkway landslide, as determined by the slide program.

Figure 9: (a) Installation of metal mesh and soil nails and (b) section of a new soldier beam retaining wall (photos courtesy of Dr. John Rockaway).

Figure 10: Relationship between strength parameters and factor of safety for the Ten Mile Road Landslide: (a) cohesion vs FS and (b) friction angle vs FS. Note:

Figure 11: Relationship between shear strength parameters and factor of safety for the Columbia Parkway landslide: (a) cohesion vs FS and (b) friction angle vs FS.

Figure 12: Relationship between water table location and factor of safety for the: (a) Ten Mile Road landslide and (b) Columbia Parkway landslide.

Tables

Table 1: Natural water content values for the colluvial soil samples from the landslide sites.

Table 2: Atterberg limits of the fine-grained fraction of the colluvial soil from the studied sites.

516 Table 3: Shear strength parameters for failure surface through the colluvial soil.

517

518 Table 4: Shear strength parameters for failure surface along the soil-bedrock contact.

519

520 Table 5: Slake durability index test results for the bedrock samples.

521

522

523

524

525

526

527

528

529

530

531

532

533

534

535

536

537

538

539

540

541

542

543

544

545

546

547

548

549

550

551

552

553

554

555

556

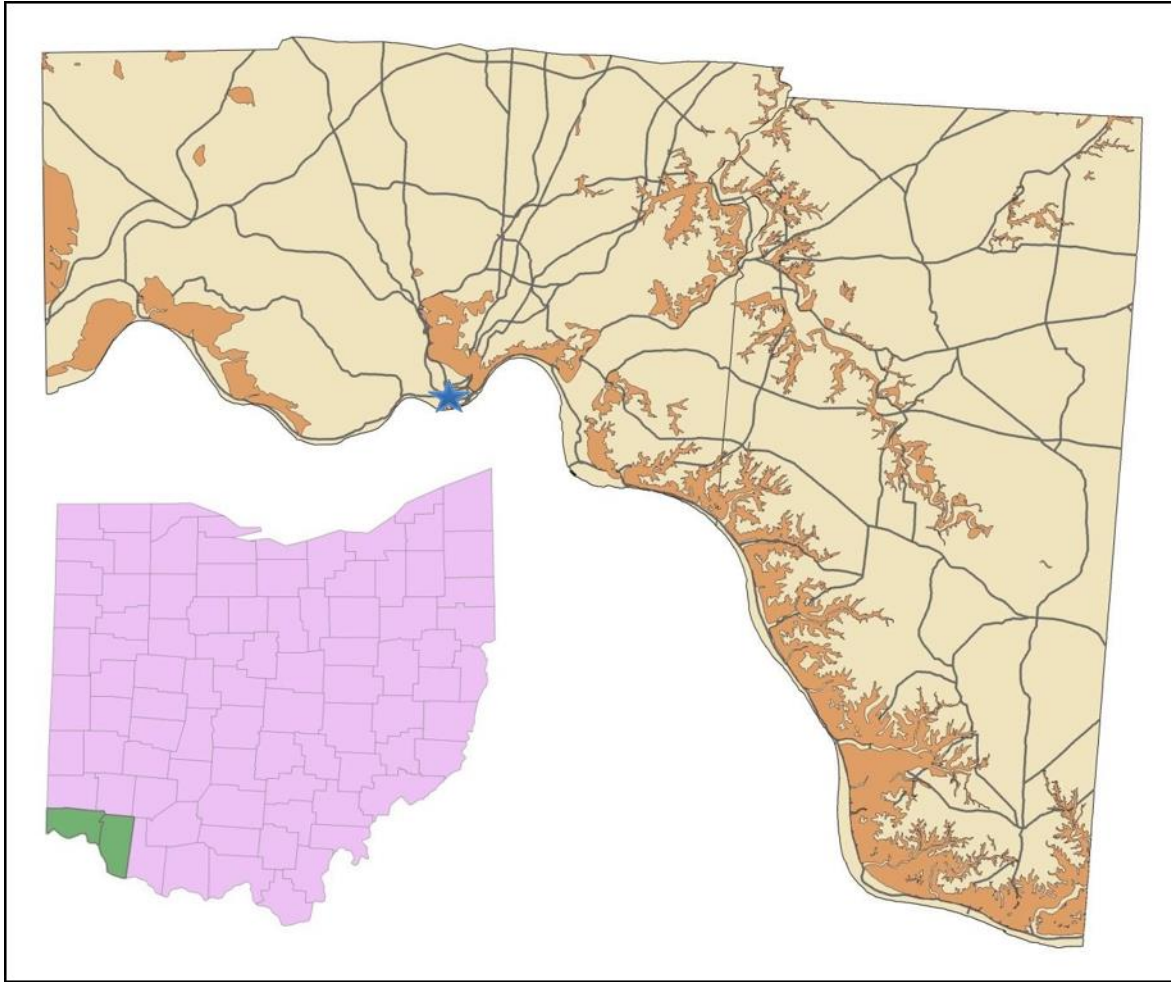
557

558

559

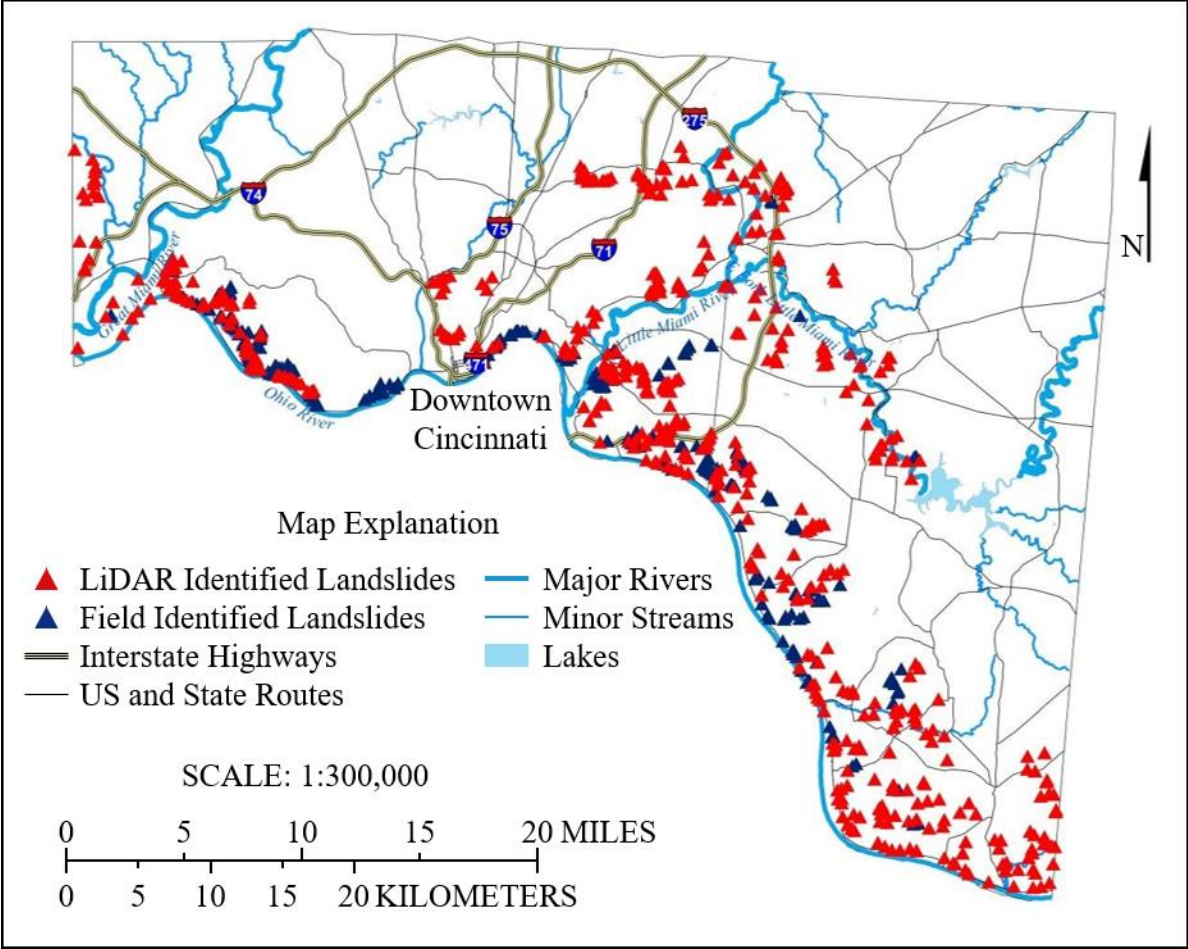
560

561



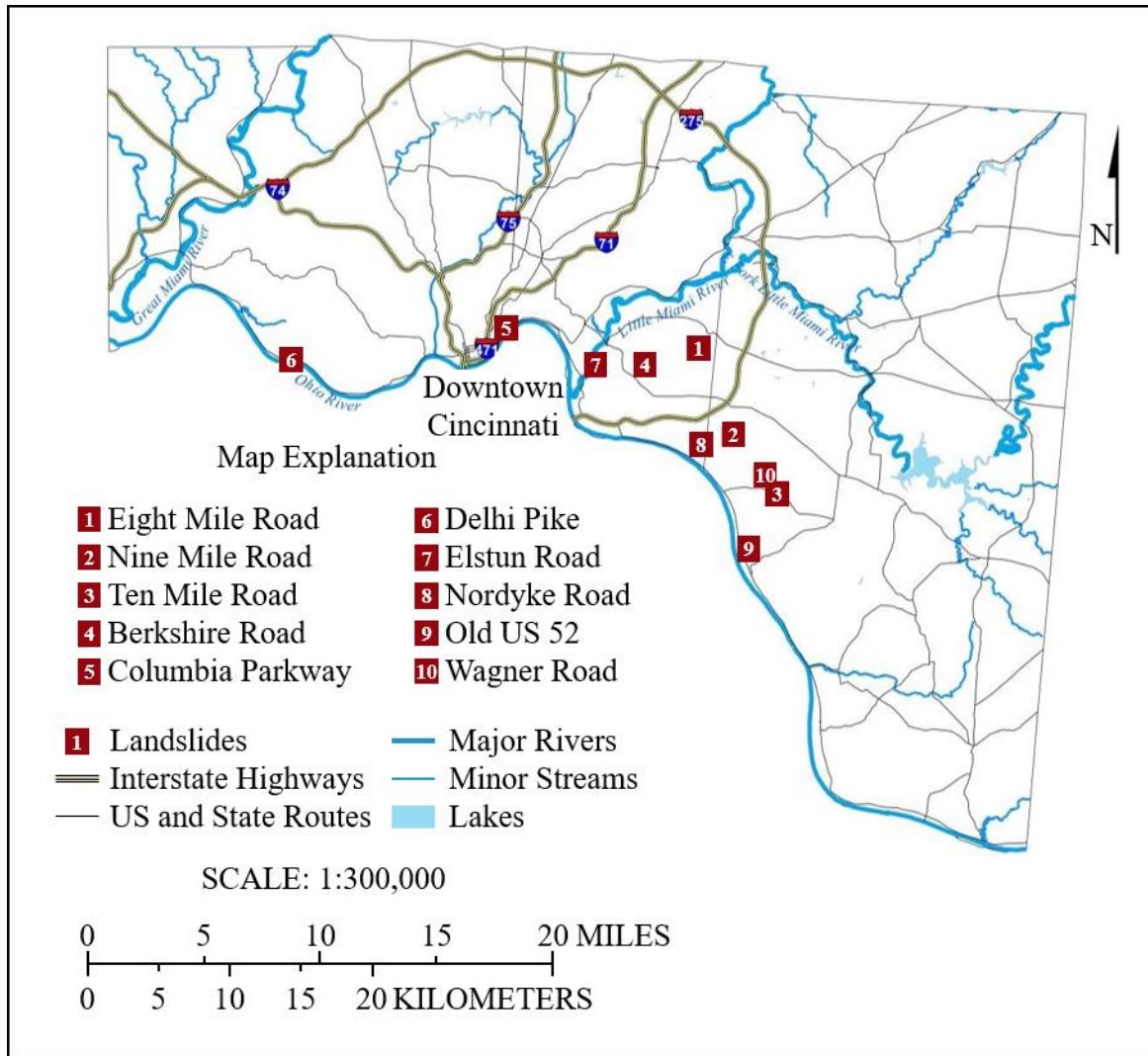
562
563
564
565
566
567
568
569
570
571

Figure 1: Map showing the extent of the Kope Formation (darker brown) in the Cincinnati area. The blue star indicates the location of downtown Cincinnati. The shaded area in the southwest corner of the Ohio map shows Hamilton (left) and Clermont (right) counties.



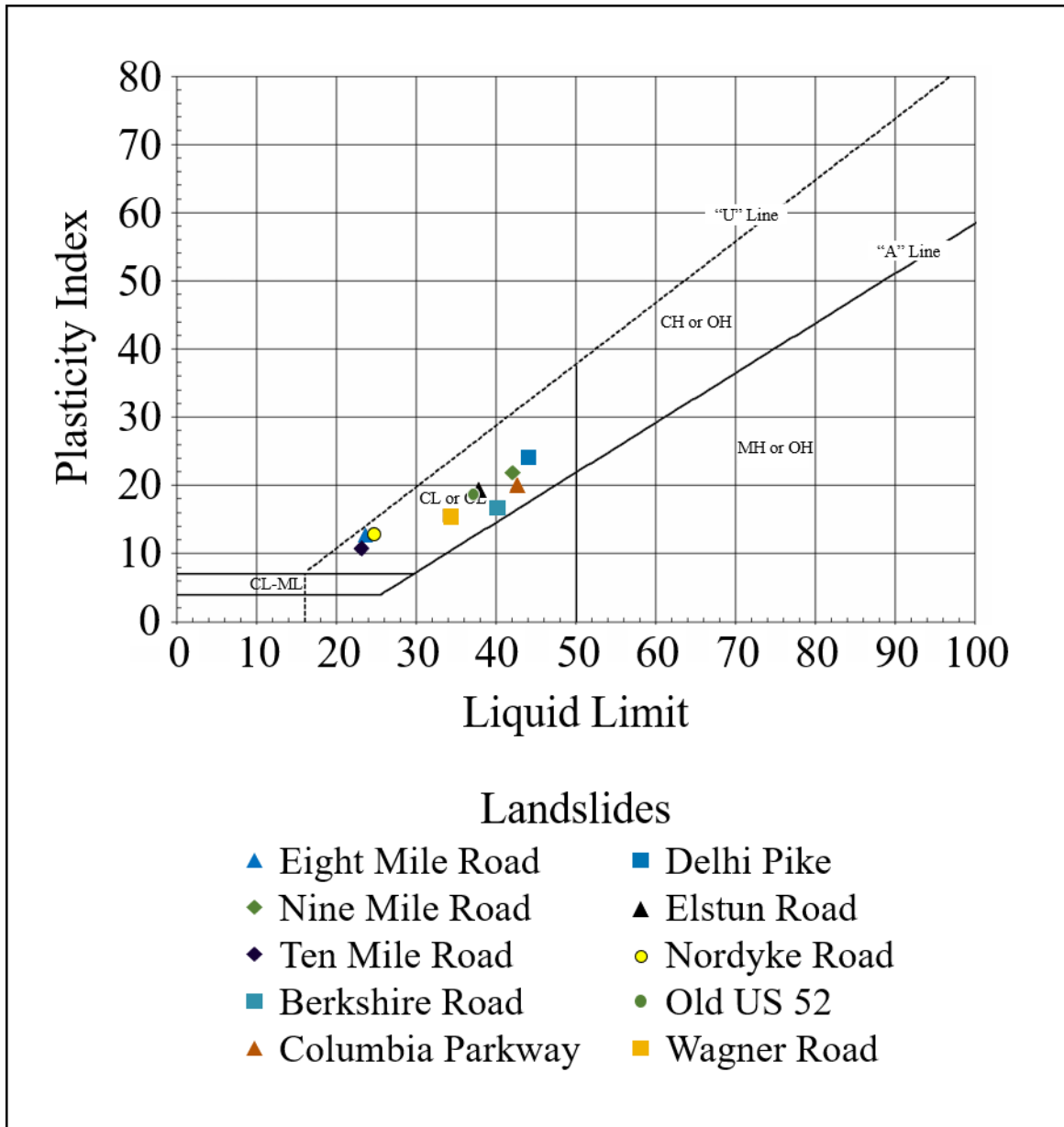
572
 573
 574
 575
 576
 577

Figure 2: Landslide inventory map for the Kope Formation and the overlying colluvial soil within the Cincinnati area.



578
579
580
581
582

Figure 3: Locations of the landslide sites selected for detailed study.



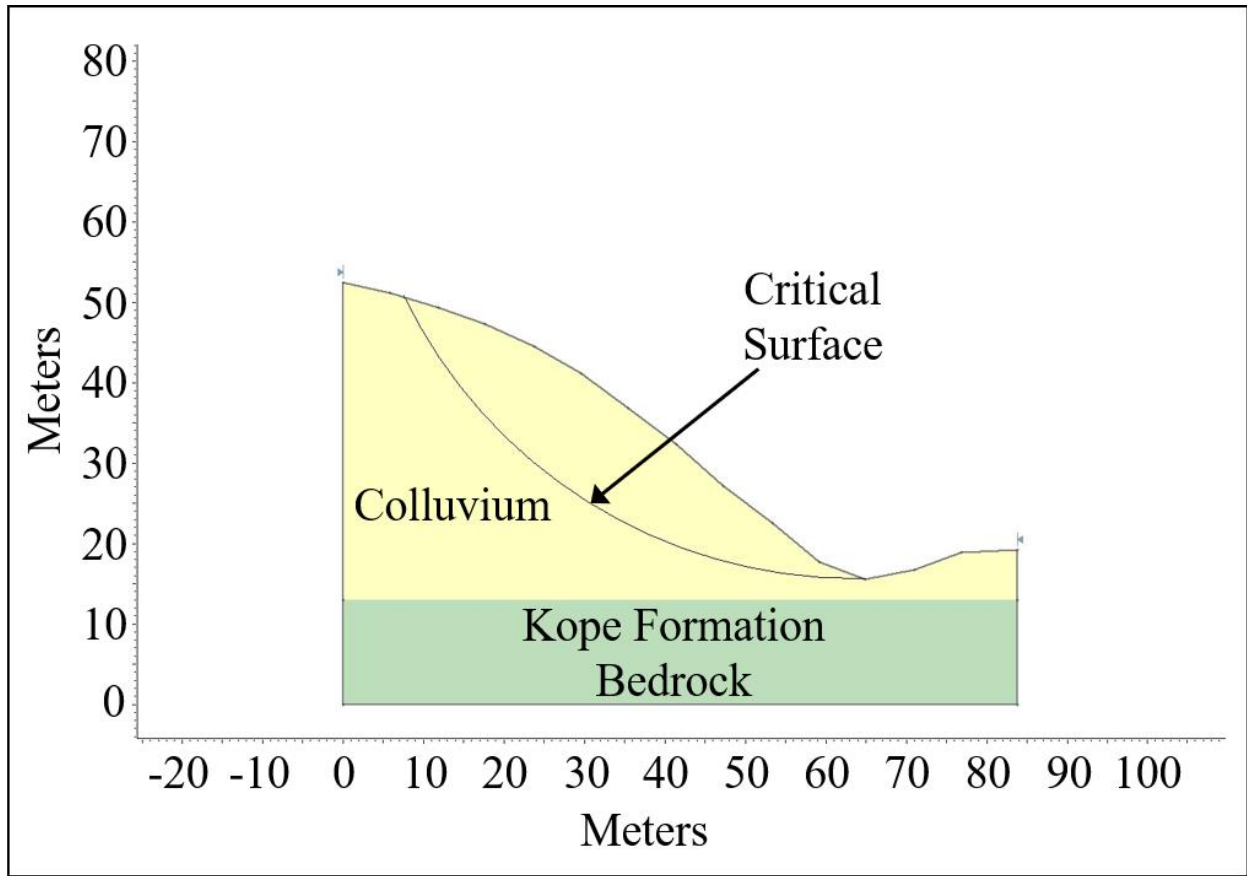
583
 584
 585
 586
 587
 588

Figure 4: Plot of Atterberg limits of the fine-grained fraction of the colluvial soils from the landslide sites on the Casagrande plasticity chart.



589
590
591
592
593
594

Figure 5: The Ten Mile Road landslide with well-developed head scarp. Notice the undercutting of the toe by a stream.



595
 596
 597
 598
 599
 600

Figure 6: Critical surface for the minimum factor of safety for dry and saturated conditions for the Ten Mile Road landslide, as determined by the Slide program.



601
602
603
604

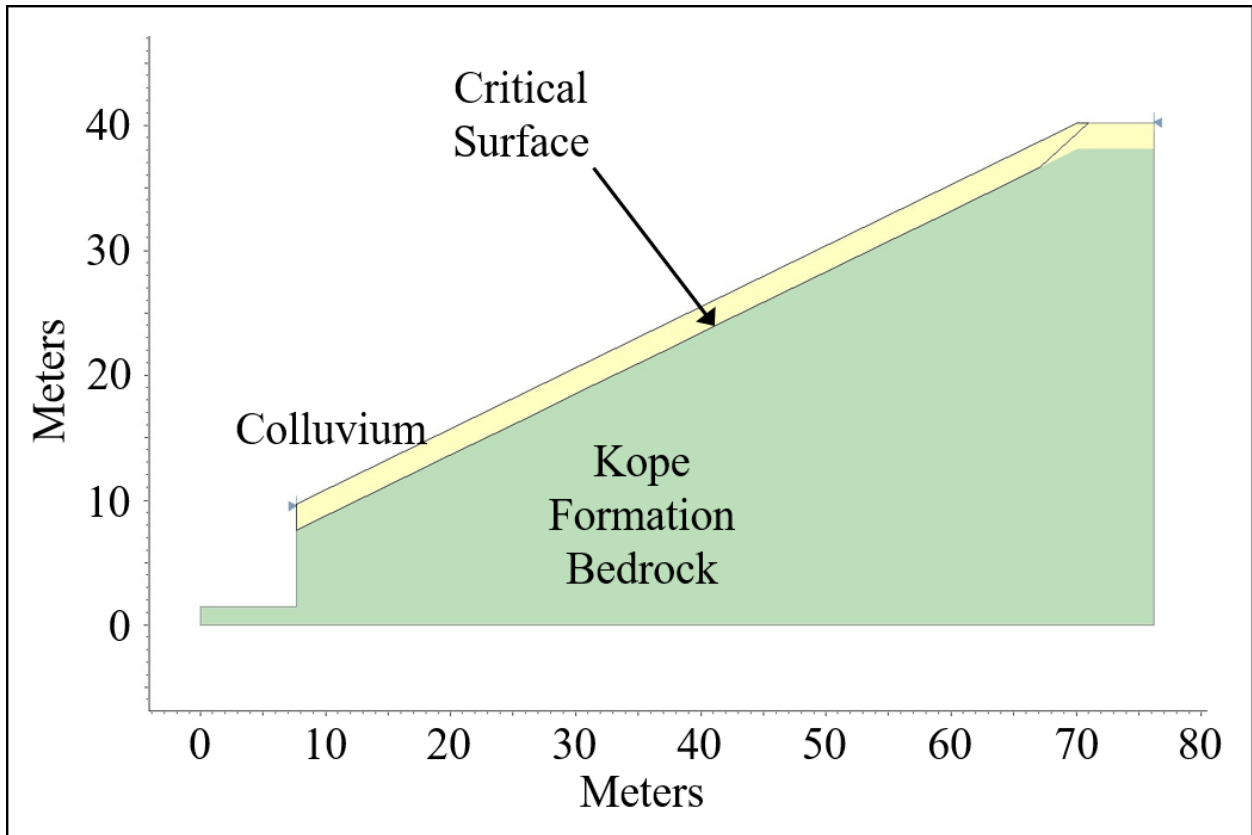
(a)



605
606
607
608
609
610
611

(b)

Figure 7: (a) Head scarp of the Columbia Parkway landslide and (b) toe of the Columbia Parkway landslide, emerging on the top of the retaining wall.



612
 613
 614
 615
 616
 617
 618
 619

Figure 8: Critical Surface for the minimum factor of safety for the Columbia Parkway landslide, as determined by the Slide program.



(a)

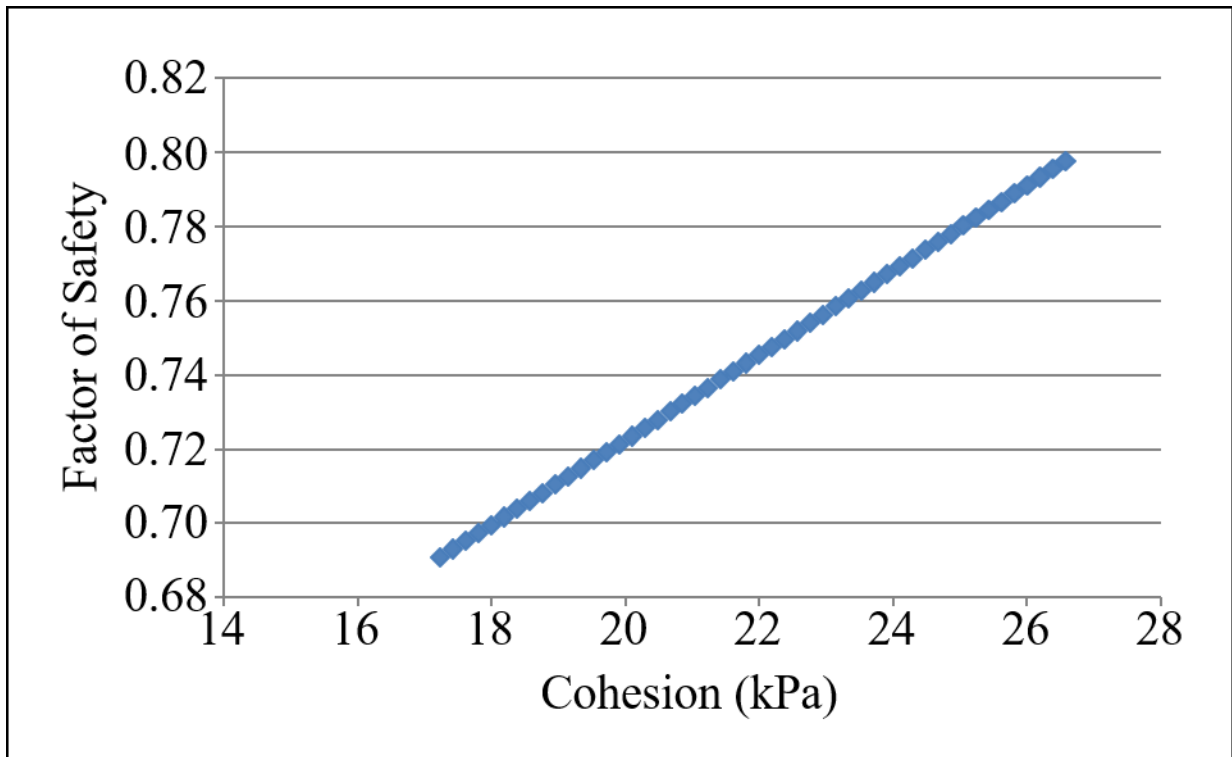
620
621
622
623



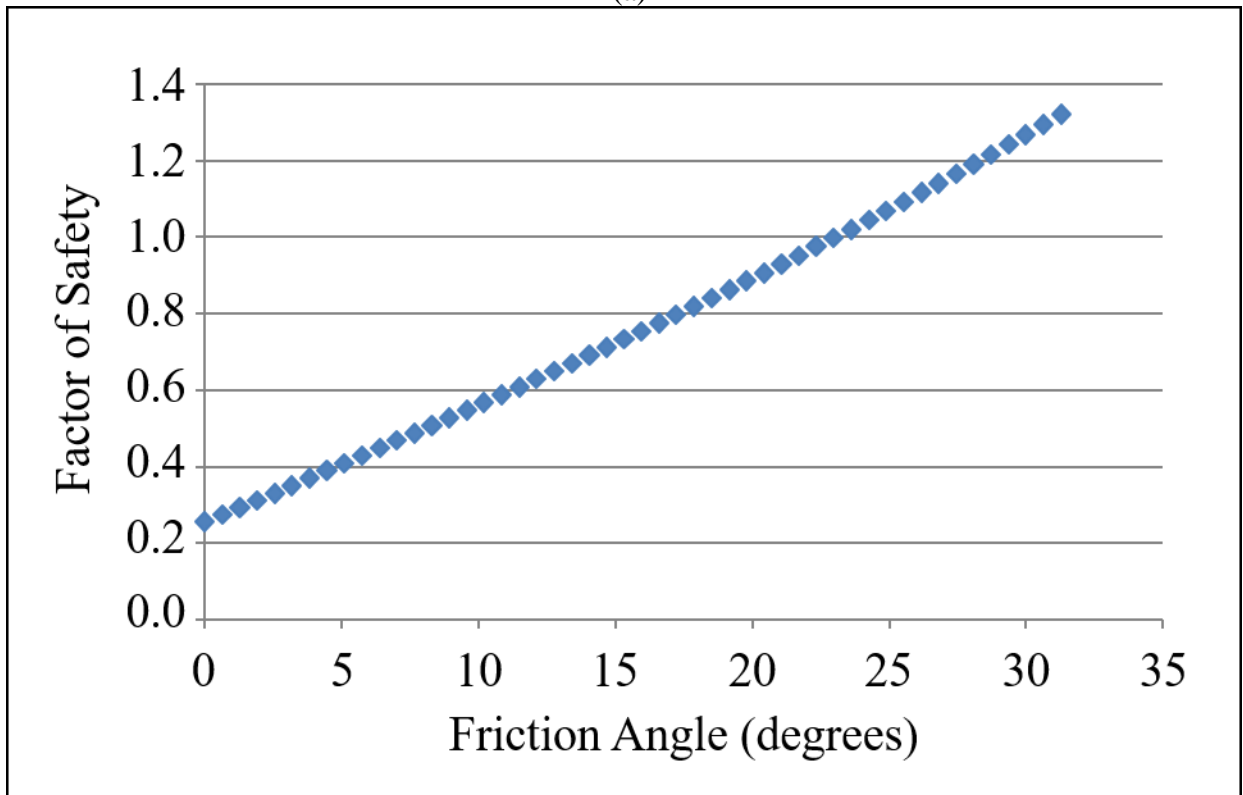
(b)

624
625
626
627
628
629

Figure 9: (a) Installation of metal mesh and soil nails and (b) section of a new soldier beam retaining wall (photos courtesy of Dr. John Rockaway).



(a)

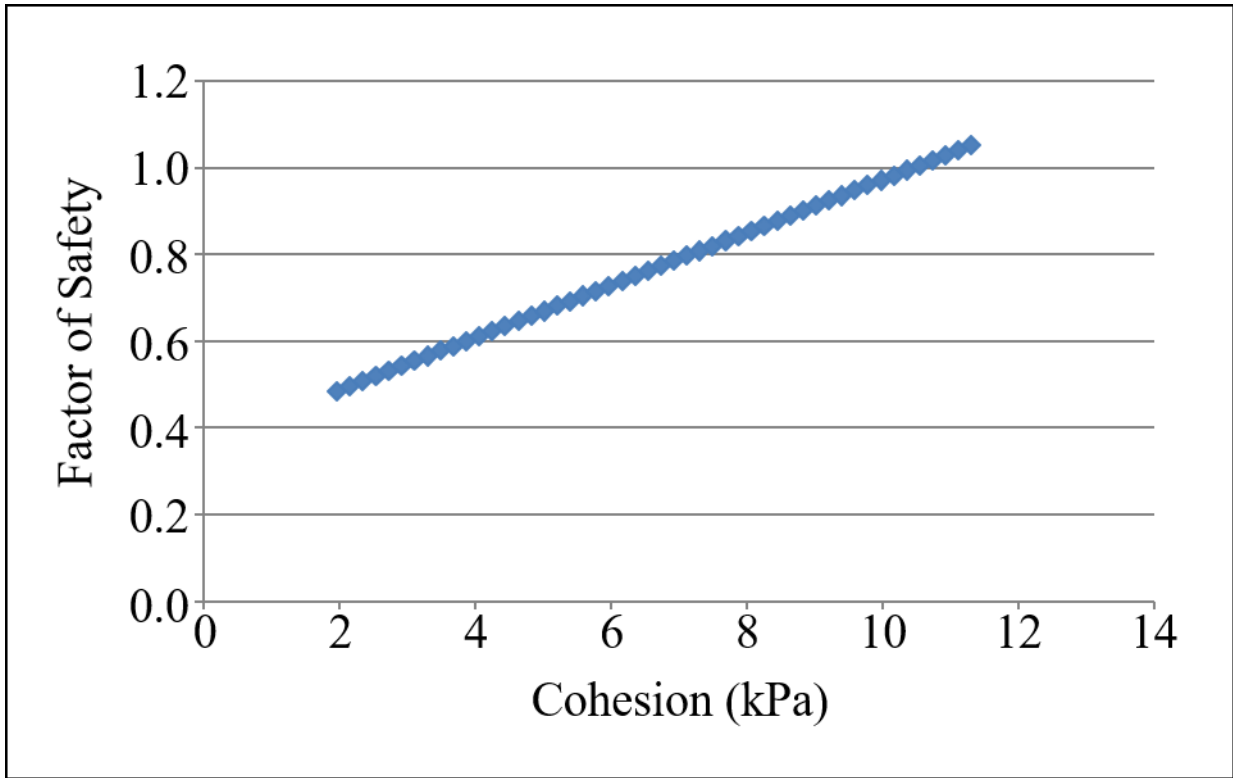


(b)

Figure 10: Relationship between strength parameters and factor of safety for the Ten Mile Road landslide: (a) cohesion vs FS and (b) friction angle vs FS.

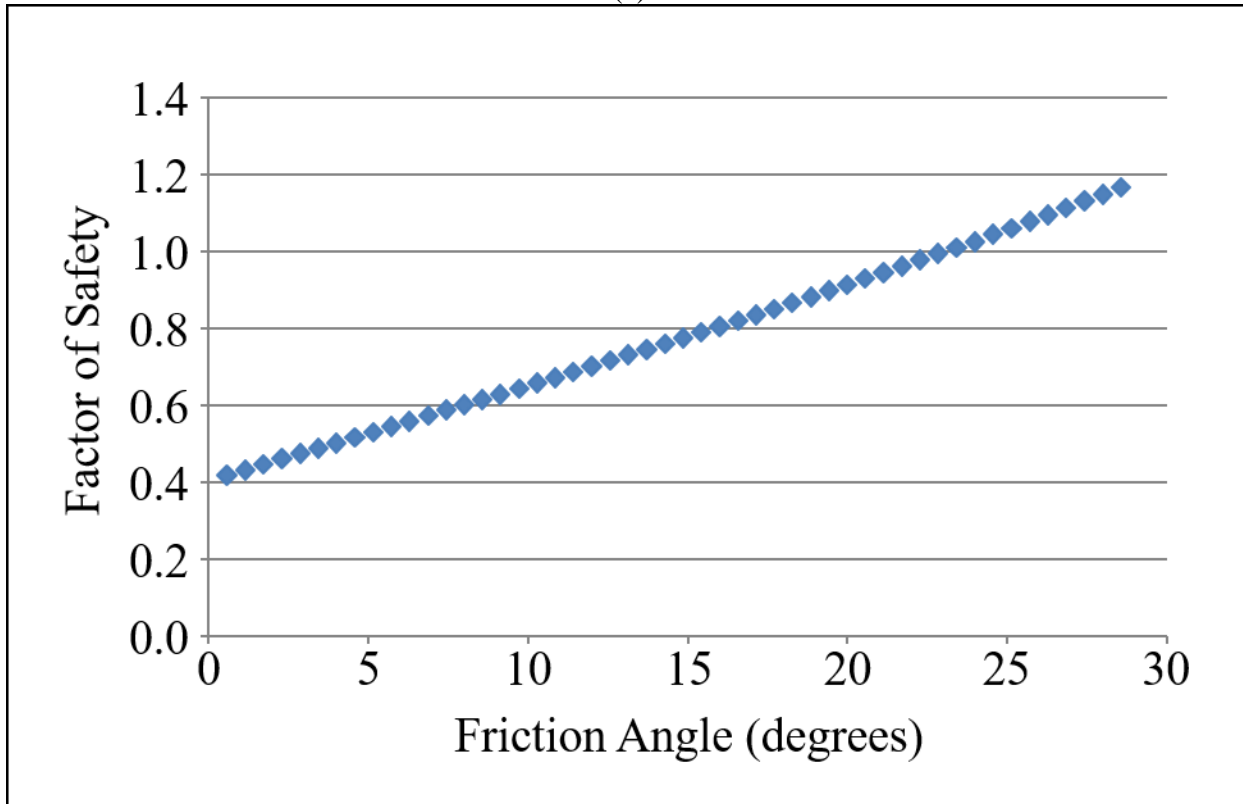
630
631

632
633
634
635
636



637
638

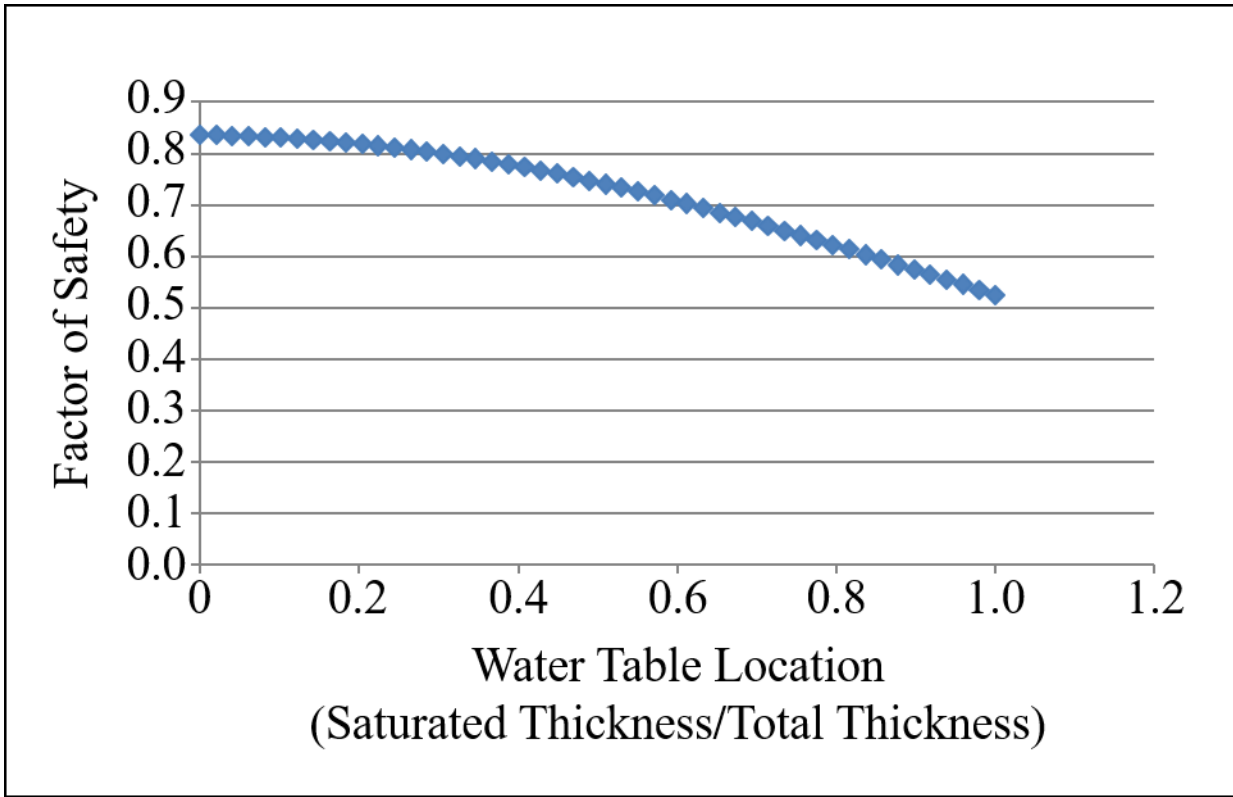
(a)



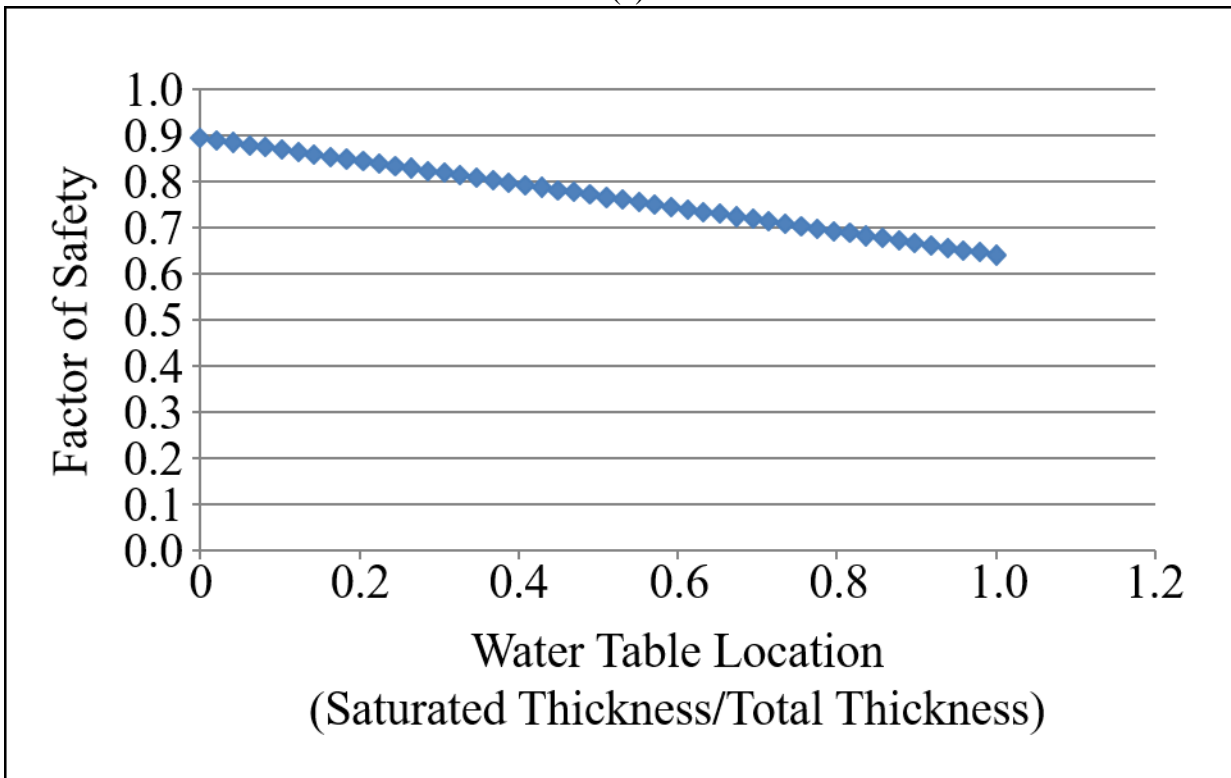
639
640

(b)

641 Figure 11: Relationship between shear strength parameters and factor of safety for the Columbia
642 Parkway landslide: (a) cohesion vs FS and (b) friction angle vs FS.



(a)



(b)

643
644

645
646
647
648

Figure 12: Relationship between water table location and factor of safety for the: (a) Ten Mile Road landslide and (b) Columbia Parkway landslide.

649 Table 1: Natural water content values for the colluvial soil samples from the landslide sites.
650

<u>Sample Location</u>	<u>Natural Water Content</u>
Eight Mile Road Landslide	13.1%
Nine Mile Road Landslide	27.1%
Ten Mile Road Landslide	13.9%
Berkshire Road Landslide	23.8%
Columbia Parkway Landslide	23.0%
Delhi Pike Landslide	25.6%
Elstun Road Landslide	18.9%
Nordyke Road Landslide	13.6%
Old US 52 Landslide	21.1%
Wagner Road Landslide	23.5%
Mean	20.4%
Median	22.0%

651

652 Table 2: Atterberg limits of the fine-grained fraction of the colluvial soil from the landslide sites.
 653
 654

Sample Location	Liquid Limit	Plastic Limit	Plasticity Index	Liquidity Index
Eight Mile Road Landslide	23.6	10.9	12.7	0.2
Nine Mile Road Landslide	41.9	20.1	21.8	0.3
Ten Mile Road Landslide	23.0	12.3	10.7	0.2
Berkshire Road Landslide	40.0	23.3	16.8	0.03
Columbia Parkway Landslide	42.6	22.5	20.1	0.02
Delhi Pike Landslide	44.0	19.8	24.2	0.2
Elstun Road Landslide	37.8	18.5	19.3	0.02
Nordyke Road Landslide	24.4	11.6	12.8	0.2
Old US 52 Landslide	37.2	18.5	18.7	0.1
Wagner Road Landslide	34.1	18.4	15.7	0.3
Mean	34.9	17.6	17.3	0.2
Median	37.5	18.5	17.8	0.2

655
 656

657
658

Table 3: Shear strength parameters for failure surface through the colluvial soil.

Sample Locations	Peak Cohesion (Kpa)	Residual Cohesion (Kpa)	Peak Friction Angle (degrees)	Residual Friction Angle (degrees)
Eight Mile Road Landslide	24.5	23.3	31.0	20.8
Ten Mile Road Landslide	27.5	22.5	33.8	15.6
Delhi Pike Landslide	33.4	24.0	23.8	17.8
Elstun Road Landslide	26.4	24.5	50.4	19.8
Nordyke Road Landslide	47.7	38.9	22.8	17.8
Old US 52 Landslide	35.2	32.7	39.4	20.3
Wagner Road Landslide	27.7	22.2	27.5	18.3
Mean	31.8	26.9	32.7	18.6
Median	27.7	24.0	31.0	18.3

659
660

661 Table 4: Shear strength parameters for failure surface along the soil-bedrock contact.
662

Sample Locations	Residual Cohesion (Kpa)	Residual Friction Angle (degrees)
Nine Mile Road Landslide	11.8	14.0
Berkshire Road Landslide	13.0	8.0
Columbia Parkway Landslide	6.8	14.6
Mean	10.5	12.2
Median	11.8	14.0

663
664

665 Table 5: Slake durability index test results for the bedrock samples from the translational
666 landslide sites.
667

Location	Slake Durability Index (Id2) (%)	Durability Rating
Berkshire Road Landslide	28.5%	Very Low
Columbia Parkway Landslide	7.1%	Very Low
Nine Mile Road Landslide	39.9%	Low

668